

# ChemComm

Accepted Manuscript



This is an *Accepted Manuscript*, which has been through the Royal Society of Chemistry peer review process and has been accepted for publication.

*Accepted Manuscripts* are published online shortly after acceptance, before technical editing, formatting and proof reading. Using this free service, authors can make their results available to the community, in citable form, before we publish the edited article. We will replace this *Accepted Manuscript* with the edited and formatted *Advance Article* as soon as it is available.

You can find more information about *Accepted Manuscripts* in the [Information for Authors](#).

Please note that technical editing may introduce minor changes to the text and/or graphics, which may alter content. The journal's standard [Terms & Conditions](#) and the [Ethical guidelines](#) still apply. In no event shall the Royal Society of Chemistry be held responsible for any errors or omissions in this *Accepted Manuscript* or any consequences arising from the use of any information it contains.



## Nanoparticle-based highly sensitive MRI contrast agents with enhanced relaxivity in reductive milieu

Received 00th January 20xx,  
Accepted 00th January 20xx

Severin J. Sigg,<sup>a</sup> Francesco Santini,<sup>bc</sup> Adrian Najer,<sup>a</sup> Pascal U. Richard,<sup>a</sup> Wolfgang P. Meier,<sup>a</sup> and Cornelia G. Palivan<sup>a\*</sup>

DOI: 10.1039/x0xx00000x

www.rsc.org/

**Current magnetic resonance imaging (MRI) contrast agents often produce insufficient contrast for diagnosis of early disease stages, and do not sense their biochemical environments. Herein, we report a highly sensitive nanoparticle-based MRI probe with  $r_1$  relaxivity up to  $51.7 \pm 1.2 \text{ mM}^{-1}\text{s}^{-1}$  (3T). Nanoparticles were co-assembled from  $\text{Gd}^{3+}$  complexed to heparin-poly(dimethylsiloxane) copolymer, and a reduction-sensitive amphiphilic peptide serving to induce responsiveness to environmental changes. The release of the peptide components leads to a  $r_1$  relaxivity increase under reducing conditions and increases the MRI contrast. In addition, this MRI probe has several advantages, such as a low cellular uptake, no apparent cellular toxicity (tested up to  $1 \text{ mM Gd}^{3+}$ ), absence of an anticoagulation property, and a high shelf stability (no increase in free  $\text{Gd}^{3+}$  over 7 months). Thus, this highly sensitive  $T_1$  MRI contrast nanoparticle system represents a promising probe for early diagnosis through possible accumulation and contrast enhancement within reductive extracellular tumour tissue.**

Magnetic resonance imaging (MRI) is a non-invasive technique that is widely used in cardiovascular, neurological, and oncological diagnostics.<sup>1</sup> Imaging is based on contrast generated by tissue-dependant variations in either the longitudinal ( $T_1$ ) or transverse ( $T_2$ ) relaxation times of the proton nuclear spins of water molecules, combined with paramagnetic contrast agents (CAs) that shorten the relaxation time of neighbouring water protons. CAs are characterized by their induced relaxivity ( $r_1$ ), defined as the change in relaxation rate ( $\Delta(1/T_1)$ ), normalized to their concentrations.<sup>2</sup> An important class of CAs is based on  $\text{Gd}^{3+}$  complexed with various ligands to avoid the intrinsic toxicity of free  $\text{Gd}^{3+}$  ions.  $\text{Gd}$ -based CAs approved for clinical use typically have an  $r_1$  of

4–5  $\text{mM}^{-1}\text{s}^{-1}$ .<sup>3</sup> These CAs are small molecules, which passively distribute after administration.<sup>4</sup> However, commercially available  $\text{Gd}$ -CAs have a low efficiency, and high doses are required for good contrast enhancement.<sup>3b,5</sup>

Three main strategies are used to improve the contrast enhancement of MRI CAs: i) modifying the ligand to increase the number of free coordination sites at the metal centre, and thus exchange rates between bulk and coordinated water, ii) increasing  $\text{Gd}$  concentrations by accumulating multiple ligands within one macromolecule, and iii) forming bulky assemblies to lower the molecular tumbling rate ( $\tau_R$ ), as both high water exchange rates and decreased molecular tumbling contribute to faster relaxation and higher MRI contrast.<sup>1</sup> In this regard, nanosized macromolecular CAs of various architectures have been reported, comprising micelles,<sup>6</sup> dendrimers,<sup>7</sup> vesicles,<sup>8</sup> and nanoparticles.<sup>1,9</sup> However, the efficiency of  $\text{Gd}$ -based CAs is influenced in a complex overall manner by various molecular and dynamic factors, and the gain in relaxivity is often far less than expected.<sup>10</sup> Also, additional introduction of specificity and responsiveness of MRI CAs to distinct environments, such as inflamed tissue or tumour microenvironments, allows specific localization and diagnosis,<sup>1,11</sup> but the production of CAs that combine high  $r_1$  relaxivity and response to physiological parameters at pathologic sites remains a major challenge.

Here we report a highly active MRI contrast agent with enhanced relaxivity in reductive milieu based on nanoparticles (NPs) resulting from co-assembly of heparin-polymers with trapped  $\text{Gd}^{3+}$  and stimuli-responsive peptides. The selection of the heparin-polymer conjugate was inspired by the strong  $\text{Gd}^{3+}$  complexing ability of the natural glycosaminoglycan heparin,<sup>12,13</sup> and the long blood circulation behaviour of heparinized NPs.<sup>14</sup> Long-circulating NPs can readily accumulate in tumour tissue via the leaky vasculature surrounding tumours (enhanced permeation and retention effect),<sup>15</sup> which increases the efficiency of cancer imaging for disease diagnosis.<sup>16</sup> Furthermore, elevated glutathione (GSH) levels in the extracellular environment of tumours, compared to healthy tissues, can be exploited as a trigger to further increase image contrast.<sup>17</sup>

<sup>a</sup> Department of Chemistry, University of Basel, Klingelbergstrasse 80, 4056 Basel, Switzerland.

<sup>b</sup> Department of Radiology, Division of Radiological Physics, University of Basel Hospital, Petersgraben 4, 4031 Basel, Switzerland.

<sup>c</sup> Department of Biomedical Engineering, University of Basel, Basel, Switzerland.

Electronic Supplementary Information (ESI) available: Materials and Methods; DLS; TEM; FT-IR; Farndale microassay; EDX; T1, T2, r1, r2 values; EPR parameters; viability and cell uptake data; and XO-assays. See DOI: 10.1039/x0xx00000x

## COMMUNICATION

ChemComm

We have now designed and synthesized an amphiphilic heparin-poly(dimethylsiloxane) (hepPDMS) block copolymer capable of self-assembling into NPs with complexation sites for  $Gd^{3+}$ . A disulfide-linked amphiphilic peptide interacts with hepPDMS-Gd via the polyhistidine sequence and co-assembles to peptide-hepPDMS-Gd NPs (p-hepPDMS-Gd-NPs). The peptide sequence ( $H_2N-H_3-X-[W-DL]_3-W-CONH_2$ ) contains a reducible linker X ( $X = -(CH_2)_2-S-S-(CH_2)_2-NH-CO-(CH_2)_2-CO-$ ) that connects the hydrophobic L-tryptophan-D-leucine repeating unit and the oligohistidine (H3SSgT).<sup>18</sup> In a reductive environment, the peptides are released, increasing the accessibility of  $Gd^{3+}$  for water molecules, and therefore increasing MRI contrast.

HepPDMS was obtained by coupling heparin polysaccharide with commercial PDMS (5kDa) via reductive amination; this yielded an average of 25 heparin repeating units per PDMS chain, as previously reported.<sup>19</sup> To create a NP-based Gd MRI CA, hepPDMS was mixed with a solution of  $GdCl_3$  (6.5 eq) in 50% ethanol at pH 7.0. NPs were formed through solvent exchange from 50% ethanol to water via dialysis, which simultaneously removed uncomplexed Gd. The hepPDMS-Gd NPs (hepPDMS-Gd-NPs) had particle size of  $51 \pm 22$  nm evaluated by dynamic light scattering (DLS), in agreement with that obtained from TEM micrographs ( $45 \pm 16$  nm) (Fig. 1A; S1). Successful complexation of Gd to the heparin-block of hepPDMS-Gd-NPs was indicated both by Fourier transform infrared spectroscopy (FTIR) and Farndale microassay (Fig. S2). The latter showed a significant decrease in accessible heparin chains on the NPs from  $1170 \pm 42$   $\mu\text{g}/\text{mL}$  (hepPDMS-NPs) to  $960 \pm 49$   $\mu\text{g}/\text{mL}$  (hepPDMS-Gd-NPs) due to partial occupation of the dye-binding sites on heparin by  $Gd^{3+}$ . The concentration of Gd complexed within the hepPDMS-NPs was determined to be 0.93 mM by inductively coupled plasma optical emission spectroscopy (ICP-OES), which is 77% of the initial Gd concentration. It demonstrates the high complexing abilities of hepPDMS, and allows the creation of a high Gd-density within the NPs that is necessary for contrast enhancement in MRI.

To introduce reduction-sensitivity to our NP-based MRI CA, the reduction-responsive amphiphilic peptide H3SSgT (0.5 mg/mL) was co-assembled with previously complexed hepPDMS-Gd to yield p-hepPDMS-Gd-NPs. The formed NPs were similar in size (DLS:  $57 \pm 38$  nm, TEM:  $43 \pm 10$  nm), and shape to those of hepPDMS-Gd-NPs (Fig. 1A,B; S1); a very small population of larger intensity weighted diameters ( $>300$  nm) was also observed, and can be attributed to purely peptidic NPs (190 nm).<sup>18</sup> Use of higher concentrations of peptide (2 mg/mL) induced formation of large aggregates along with the co-assemblies (Fig. S3), and thus further characterization of co-assemblies was performed with a lower peptide concentration (0.5 mg/mL). Energy dispersive X-ray spectroscopy (EDX) analysis showed co-localization of Gd and sulfur (from the disulfide in the peptide and from hepPDMS) within the particles (Fig. S4). The expected interaction of the histidine residues of the peptide with the heparin block of hepPDMS when co-assembled was analyzed by Farndale microassays; the co-assembled peptide decreased the accessibility of heparin from  $1020 \pm 82$   $\mu\text{g}/\text{mL}$  to  $760 \pm 85$   $\mu\text{g}/\text{mL}$ . Since the assay

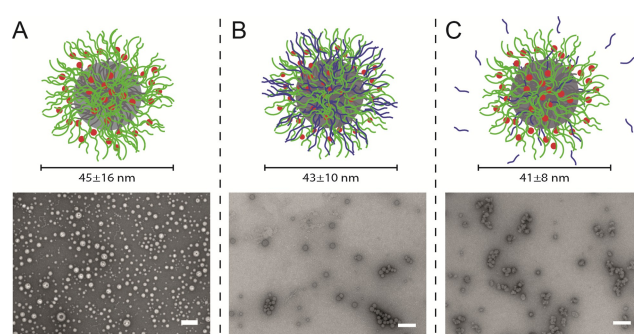


Fig. 1 Schematic representation and TEM micrographs of (A) hepPDMS-Gd-NPs (B) p-hepPDMS-Gd-NPs (-DTT), and (C) p-hepPDMS-Gd-NPs (+DTT). Sizes obtained by TEM are indicated. Scale bars: 200 nm.

monitors the accessible heparin, these values represent the situation on the surfaces

of the NPs rather than in their core, and also demonstrate steric hindrance originating from the co-assembled peptides.

Zeta potential measurements revealed slightly different values ( $-55.0 \pm 0.5$  mV) for p-hepPDMS-Gd-NPs and NPs assembled without peptide ( $-58.0 \pm 0.3$  mV), but these are rather small for heparin is the most negatively charged biological macromolecule.<sup>20</sup> At H3SSgT/hepPDMS-Gd ratios suitable for co-assembly, the number of histidines is insufficient to neutralize the charge of heparin, and the NPs are thus highly negatively charged. The preservation of heparin characteristics on the nanoparticle surfaces after Gd-complexation and co-assembly with peptides provides the desired properties for prolonged blood circulation time,<sup>14</sup> which is required for accumulation in tumour regions via the enhanced permeation and retention effect, and subsequent contrast enhancement for MRI diagnostics.<sup>16</sup> For assessing size and morphology changes of p-hepPDMS-Gd-NPs upon reductive stimuli, they were treated with 10 mM dithiothreitol (DTT) in HEPES buffer at pH 7.2. This resulted in slightly decreased diameters ( $44 \pm 19$  nm by DLS,  $41 \pm 8$  nm by TEM) compared to hepPDMS-Gd-NPs (Fig. 1A,C; S1).

The suitability of these Gd-complexing NPs as MRI contrast agents was assessed in comparison with commercial Gd 1,4,7,10-tetraazacyclododecane-1,4,7,10-tetraacetic acid (Gd-DOTA/Dotarem®), which is one of the most frequently applied CA in clinical MRI. At a field of 3T, Gd-DOTA had  $T_1$  relaxation times in a range of 1360 ms at 0.10 mM Gd and 213 ms at 0.99 mM Gd (Fig. 2A, Table S1), resulting in a  $r_1$  relaxivity of  $4.5 \pm 0.1$   $\text{mM}^{-1}\text{s}^{-1}$  (Fig. 2C, Table S1), which is in agreement with literature values.<sup>21</sup> However, when Gd was complexed within hepPDMS NPs, the water relaxivity increased to  $51.7 \pm 1.2$   $\text{mM}^{-1}\text{s}^{-1}$ , which is more than an order of magnitude higher than for Gd-DOTA. This can be attributed mainly to decreased tumbling rates of the large NPs combined with different binding characteristics which create faster exchange rates at the metal centres. When co-assembled with H3SSgT, p-hepPDMS-Gd-NPs the  $r_1$  of  $44.2 \pm 1.5$   $\text{mM}^{-1}\text{s}^{-1}$  (Fig. 2C, Table S1) was lower than for the purely hepPDMS-Gd-based nanoparticles. This may be because the close arrangement of the peptidic histidines to the heparin block of the copolymer increases the density of

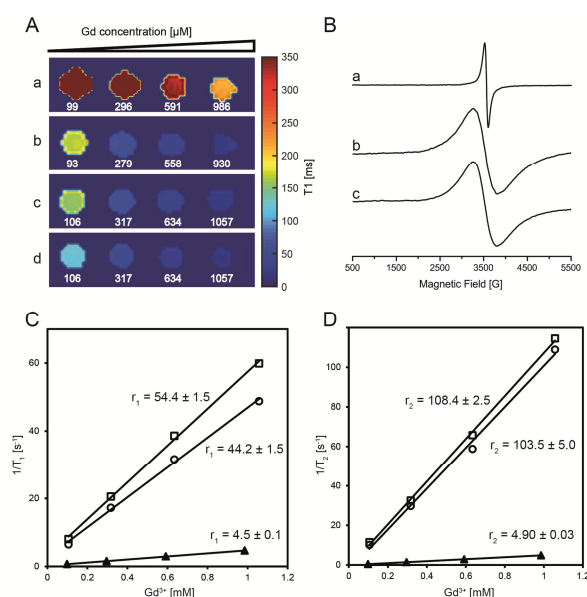


**Fig. 2** (A)  $T_1$  weighted MR image of a) Gd-DOTA, b) hepPDMS-Gd-NPs, c) p-hepPDMS-Gd-NPs (-DTT), and d) p-hepPDMS-Gd-NPs (+DTT); concentration of each sample in  $\mu\text{M}$  is given in white. (B) EPR spectra of a) Gd-DOTA, b) hepPDMS-Gd-NPs, c) p-hepPDMS-Gd-NPs (-DTT). (C) and (D)  $r_1$  and  $r_2$  relaxivity curves of p-hepPDMS-Gd (+DTT) (squares), p-hepPDMS-Gd (-DTT) (circles), and Gd-DOTA (triangles);  $r_1$  and  $r_2$  relaxivities are given in  $\text{mM}^{-1}\text{s}^{-1}$ . Detailed discussion of this figure is available in ESI

the co-assembled particles, thereby sterically hindering water access and coordination to the metal centres.

After addition of the reducing agent (DTT) an increase in  $r_1$  of about 20% to  $54.4 \pm 1.5 \text{ mM}^{-1}\text{s}^{-1}$  was obtained (Fig. 2C, Table S1), a value close to that of NPs assembled from hepPDMS-Gd alone. This increase in relaxivity in a reductive environment can be used to obtain increased contrast for cancerous tissue based on the elevated GSH-levels in extracellular space of tumours.<sup>17</sup> Similar trends were also observed in  $T_2$  relaxation rates for the NPs compared to Gd-DOTA. For hepPDMS-Gd-NPs a transverse relaxation rate,  $r_2$ , of  $162.6 \pm 17.8 \text{ mM}^{-1}\text{s}^{-1}$  was obtained, and this decreased to  $103.5 \pm 5.0 \text{ mM}^{-1}\text{s}^{-1}$  for particles co-assembled with H3SSgT and  $108.4 \pm 2.5 \text{ mM}^{-1}\text{s}^{-1}$  after DTT addition (Fig. 2D, Table S1). These values are more than one order of magnitude higher than for Gd-DOTA ( $4.90 \pm 0.03 \text{ mM}^{-1}\text{s}^{-1}$ ) (a comparison of  $r_1$  relaxivities with experimental nanosized CAs is available in the ESI).

To gain more insight into the behaviour of these Gd-nanoparticles we used electron paramagnetic resonance (EPR) spectroscopy to calculate values of the transverse electronic relaxation rates,  $1/T_{2e}$ . Whilst the EPR spectra of Gd-DOTA, hepPDMS-Gd-NP and p-hepPDMS-Gd-NPs all have g-values around 2.00, those of both Gd-NPs have very broad lines and thus significantly different  $1/T_{2e}$  values from Gd-DOTA (Fig. 2B, Table S2). At a magnetic field of 0.34 T  $1/T_{2e}$  for Gd-DOTA was calculated as  $1.31 \times 10^9 \text{ s}^{-1}$ ,<sup>22</sup> whereas the corresponding values for hepPDMS-Gd-NPs and p-hepPDMS-Gd-NPs were  $6.56 \times 10^9 \text{ s}^{-1}$ , and  $5.98 \times 10^9 \text{ s}^{-1}$ , respectively. The decreased  $T_{2e}$  can be explained by intramolecular dipole-dipole interactions between Gd ions in the NPs,<sup>23</sup> the distribution of multiple Gd sites within the NPs and a slower rotational correlation time

due to the size difference. These results are in agreement with previous reports that indicated increased proton relaxivity associated with rigid micelle-like structures.<sup>24</sup> The slight difference in  $1/T_{2e}$  between hepPDMS-Gd-NP and p-hepPDMS-Gd-NP is due to the shielding effect of the co-assembled peptide.

The high relaxivities  $r_1$  exhibited by hepPDMS-Gd-NPs, p-hepPDMS-Gd-NPs, and DTT-treated p-hepPDMS-Gd-NPs indicate their potential for providing high contrast MRI. However, in order to be applicable *in vivo*, CAs should have no cellular toxicity. Thus we evaluated cell viability with HeLa cells, and various concentrations of p-hepPDMS-Gd-NPs, hepPDMS-Gd-NPs, and commercial Gd-DOTA. None of the particles showed any cellular toxicity up to 1.0 mM Gd (Fig. S5A). Since the absence of cellular toxicity could be the consequence of low cellular uptake as a result of the highly negative surface charge on our NPs, this was tested by incubating hepPDMS-Gd and p-hepPDMS-Gd nanoparticles with HeLa cells, then washing, digesting and quantifying the Gd content using ICP-OES; only small uptake of 2.8% and 5.4%, respectively was determined (Fig. S5B). This is advantageous because the desired long-circulation time within the blood stream, requires low cellular uptake, and subsequent fast removal from the body.

Leakage of free  $\text{Gd}^{3+}$  ions from complexes/assemblies is associated with toxicity and represents another hurdle for translation towards an *in vivo* applicable MRI CA. Therefore, we quantified free  $\text{Gd}^{3+}$  in solution using a xylenol orange colorimetric assay. HepPDMS-Gd-NPs and p-hepPDMS-Gd-NPs showed that 8.5% and 5.9%, respectively of the Gd was present as free  $\text{Gd}^{3+}$ . The level of free  $\text{Gd}^{3+}$  was unchanged by keeping the NPs for seven months at room temperature, although the NP partly rearranged to larger sizes, particularly for peptide co-assemblies (Fig. S6). This behaviour can be explained by slow sedimentation and subsequent aggregation of the NPs. Stability of the NPs was also investigated by incubation in cell growth media Gd levels remained below the detection limit of about  $1 \mu\text{M}$  after seven days, although the sensitivity was limited by interaction of the colorimetric assay with the culture media. This concentration is considered noncritical since concentrations of 0.1–0.3 mmol/kg<sup>25</sup> are normally applied for commercial MRI CAs, which have an  $r_1$  of 4–5  $\text{mM}^{-1}\text{s}^{-1}$  and LD50 values for Gd of 0.5 mmol/kg in rats.<sup>26</sup> Heparin is known to exhibit anticoagulation properties, which are undesirable for MRI applications. Therefore, the anticoagulation activity of our system was evaluated using standard anti-Xa assays. It was found to be below the limit of detection of the assay (<0.1 U/mL) for hepPDMS-Gd-NPs and p-hepPDMS-Gd-NPs at concentrations of 700 and 580  $\mu\text{g}/\text{ml}$  of accessible heparin (equivalent to 135 and 110 U/ml), respectively. Thus the anticoagulation ability of heparin is greatly reduced by conjugation to PDMS and subsequent NP formation.

Responsive, high-relaxivity MRI contrast agents are in high demand for clinical diagnostics, and in this respect, p-hepPDMS-Gd-NPs fulfil numerous key criteria for use as responsive high relaxivity CAs, and have an  $r_1$  relaxivity (44.2

$\text{mM}^{-1}\text{s}^{-1}$ ) that is tenfold higher than Gd-DOTA ( $4.5 \text{ mM}^{-1}\text{s}^{-1}$ ), which is currently considered to be the gold standard. Furthermore, addition of a reducing agent increased  $r_1$  by about 20% to  $54.4 \text{ mM}^{-1}\text{s}^{-1}$ . Thus the high values of  $r_1$  allow use of significantly lower doses of our NPs, whilst preserving high contrast for diagnostics. In addition, the triggered enhancement of  $r_1$  enables higher contrast generation in regions with increased reduction potential, such as cancerous tissue. *In vitro* cell assays demonstrated low cellular uptake, and the absence of cellular toxicity of the assembled NPs (comparable values for Gd-DOTA and NPs). Furthermore, they did not show any anticoagulation activity *in vitro* and were stable over seven months at room temperature. Thus our novel approach using natural complexing ligands for developing highly sensitive NP-based MRI CAs, which additionally have increased relaxivity in reducing environments, offers a promising direction for future optimization and application of these NPs.

Financial support by Gebert Rűf Foundation (GRS-048/11), SNSF, and NCCR-MSE are kindly acknowledged. S.J.S. thanks FAG-Basel for a fellowship, Dr. Viktoriia Postupalenko for toxicity assays, and Dr. Jason Duskey for discussions. Prof. Seebeck (Uni Basel) is acknowledged for access to the peptide synthesizer, Gabi Persy (Uni Basel) for TEM micrographs, Eva Bieler for SEM and EDX, and the Zentrum for microscopy Basel for access and support. Prof. Dimitrios Tsakiris (Basel University Hospital) is acknowledged for anticoagulation assays, Judith Kobler Waldis (Uni Basel) for ICP-OES analyses and Dr. Bernard A. Goodman for editing the manuscript.

## Notes and references

- J. Tang, Y. Sheng, H. Hu and Y. Shen, *Prog. Polym. Sci.*, 2013, **38**, 462-502.
- P. Caravan, *Chem. Soc. Rev.*, 2006, **35**, 512-523.
- (a) V. C. Pierre, M. J. Allen and P. Caravan, *J. Biol. Inorg. Chem.*, 2014, **19**, 127-131; (b) E. J. Werner, A. Datta, C. J. Jocher and K. N. Raymond, *Angew. Chem., Int. Ed.*, 2008, **47**, 8568-8580.
- P. Caravan, J. J. Ellison, T. J. McMurry and R. B. Lauffer, *Chem. Rev. (Washington, DC, U. S.)*, 1999, **99**, 2293-2352.
- P. J. Klemm, W. C. Floyd, 3rd, D. E. Smiles, J. M. Frechet and K. N. Raymond, *Contrast Media Mol. Imaging*, 2012, **7**, 95-99.
- (a) K. Shiraishi, K. Kawano, Y. Maitani and M. Yokoyama, *J. Controlled Release*, 2010, **148**, 160-167; (b) K. Shiraishi, K. Kawano, T. Minowa, Y. Maitani and M. Yokoyama, *J. Controlled Release*, 2009, **136**, 14-20.
- (a) M. R. Longmire, M. Ogawa, P. L. Choyke and H. Kobayashi, *Wiley Interdiscip. Rev.: Nanomed. Nanobiotechnol.*, 2014, **6**, 155-162; (b) M. Ye, Y. Qian, J. Tang, H. Hu, M. Sui and Y. Shen, *J. Controlled Release*, 2013, **169**, 239-245.
- (a) Z. Cheng, A. Al Zaki, I. W. Jones, H. K. Hall, Jr., C. A. Aspinwall and A. Tsourkas, *Chem. Commun. (Cambridge, U. K.)*, 2014, **50**, 2502-2504; (b) P. M. Winter, J. Pearce, Z. Chu, C. M. McPherson, R. Takigiku, J. H. Lee and X. Qi, *Magn. Reson. Imaging*, 2015, **41**, 1079-1087; (c) Y. Chen, Q. Zhu, Y. Tian, W. Tang, F. Pan, R. Xiong, Y. Yuan and A. Hu, *Polym. Chem.*, 2015, **6**, 1521-1526.
- (a) H. Korkusuz, K. Ulbrich, K. Welzel, V. Koeberle, W. Watcharin, U. Bahr, V. Chernikov, T. Knobloch, S. Petersen, F. Huebner, H. Ackermann, S. Gelperina, W. Kromen, R. Hammerstingl, J. Hauptenthal, F. Gruenwald, J. Fiehler, S. Zeuzem, J. Kreuter, T. J. Vogl and A. Piiper, *Mol. Imaging Biol.*, 2013, **15**, 148-154; (b) P. Mi, D. Kokuryo, H. Cabral, M. Kumagai, T. Nomoto, I. Aoki, Y. Terada, A. Kishimura, N. Nishiyama and K. Kataoka, *J. Controlled Release*, 2014, **174**, 63-71; (c) J. Zhu, B. Zhang, J. Tian, J. Wang, Y. Chong, X. Wang, Y. Deng, M. Tang, Y. Li, C. Ge, Y. Pan and H. Gu, *Nanoscale*, 2015, **7**, 3392-3395; (d) J. Zhu, J. Wang, X. Wang, J. Zhu, Y. Yang, J. Tian, W. Cui, C. Ge, Y. Li, Y. Pan and H. Gu, *J. Mater. Chem. B*, 2015, **3**, 6905-6910.
- V. S. Vexler, O. Clément, H. Schmitt-Willich and R. C. Brasch, *J. Magn. Reson. Imaging*, 1994, **4**, 381-388.
- G. L. Davies, I. Kramberger and J. J. Davis, *Chem. Commun. (Cambridge, U. K.)*, 2013, **49**, 9704-9721.
- D. L. Rabenstein, J. M. Robert and J. Peng, *Carbohydr. Res.*, 1995, **278**, 239-256.
- M. Taupitz, N. Stolzenburg, M. Ebert, J. Schnorr, R. Hauptmann, H. Kratz, B. Hamm and S. Wagner, *Contrast Media Mol. Imaging*, 2013, **8**, 108-116.
- (a) C. Passirani, G. Barratt, J.-P. Devissaguet and D. Labarre, *Pharm. Res.*, 1998, **15**, 1046-1050; (b) J. Zhang, M. C. Shin, A. E. David, J. Zhou, K. Lee, H. He and V. C. Yang, *Mol. Pharm.*, 2013, **10**, 3892-3902.
- (a) Y. Matsumura and H. Maeda, *Cancer Res.*, 1986, **46**, 6387-6392; (b) J. Fang, H. Nakamura and H. Maeda, *Adv. Drug Delivery Rev.*, 2011, **63**, 136-151.
- (a) H. Daldrup, D. M. Shames, M. Wendland, Y. Okuhata, T. M. Link, W. Rosenau, Y. Lu and R. C. Brasch, *Am. J. Roentgenol.*, 1998, **171**, 941-949; (b) Z. Zhou and Z. R. Lu, *Wiley Interdiscip. Rev.: Nanomed. Nanobiotechnol.*, 2013, **5**, 1-18.
- (a) C. L. Grek and K. D. Tew, *Curr. Opin. Pharmacol.*, 2010, **10**, 362-368; (b) L. Chaiswing and T. D. Oberley, *Antioxid. Redox Signaling*, 2009, **13**, 449-465.
- S. J. Sigg, V. Postupalenko, J. T. Duskey, C. G. Palivan and W. Meier, *Biomacromolecules*, 2016, **17**, 935-945.
- A. Najer, D. Wu, A. Bieri, F. Brand, C. G. Palivan, H.-P. Beck and W. Meier, *ACS Nano*, 2014, **8**, 12560-12571.
- Z. Yang, Q. Tu, J. Wang and N. Huang, *Biomaterials*, 2012, **33**, 6615-6625.
- A. J. L. Villaraza, A. Bumb and M. W. Brechbiel, *Chem. Rev. (Washington, DC, U. S.)*, 2010, **110**, 2921-2959.
- F. A. Dunand, A. Borel and L. Helm, *Inorg. Chem. Commun.*, 2002, **5**, 811-815.
- K. E. Kellar, P. M. Henrichs, R. Hollister, S. H. Koenig, J. Eck and D. Wei, *Magn. Reson. Med.*, 1997, **38**, 712-716.
- G. M. Nicolle, É. Tóth, H. Schmitt-Willich, B. Radüchel and A. E. Merbach, *Chem. - Eur. J.*, 2002, **8**, 1040-1048.
- M. A. Perazella, *Clin. J. Am. Soc. Nephrol.*, 2009, **4**, 461-469.
- R. B. Lauffer, *Chem. Rev. (Washington, DC, U. S.)*, 1987, **87**, 901-927.